Roque-Ruiz and Reyes-López, J Material Sci Eng 2016, 6:1
DOI: 10.4172/2169-0022.1000305

Journal of Material Sciences & Engineering

Commentary Open Access

Synthesis of α-Al_2O_3 Nanopowders at Low Temperature from Aluminum Formate by Combustion Process

Roque-Ruiz JH and Reyes-López SY*

Department of Biological Sciences, Institute of Biomedical Sciences, Autonomous University of Ciudad Juárez, Surrounding Ring of PRONAF and Stockholm s/n, Mexico

Abstract

Chemical synthesis results in the most convenient route to produce ceramics nanoparticles. The methodology used consists in the formation of a sol from organometallic precursors. Two different fuels, ovalbumin and urea, along with aluminum formate were used to prepare nano alpha-alumina powder. Different fuel to oxidizer ratios and different percentage combination of two fuels were used to prepare six samples. In all samples, nanoscale particle size was obtained. The addition of urea and ovalbumin promotes amorphous character below 800°C. With the fuel approach, crystallinity can be enhanced easily, by calcination of powder product at low temperature around 1050°C. The methodology has capability to produce nanophase alumina powder with wide range of particles size 40-80 nm. Therefore the use of this precursor simplifies the process and provides another alternative process for economical synthesis of crystalline alumina.

Keywords: Combustion synthesis; Nanoceramics; Aluminum formate; Alumina; Organometallic

Introduction

Alumina (Al_2O_3) is one of the most important ceramic materials used for industrial applications. Several alumina polymorphs have been used for fabrication of catalysts and catalysts supports, adsorbent materials, and coatings [1]. This ceramic presents high mechanical strength and hardness, as well as high thermal and corrosion resistance. Nanostructured ceramics possess enhanced mechanical properties such as strength and toughness, compared to monolithic materials [2].

Producing α-alumina nanoparticles is a difficult process for two main reasons. First, α-alumina is the most stable polymorph of this ceramic, and once it is synthesized the particle size increases quickly. Also, several particles tend to agglomerate during dehydration processes [1,3]. Commonly, nanometric alumina powders are obtained by different methods, such as ball milling, precipitation, hydrothermal synthesis and vapor phase reaction. Nevertheless, such methods have several disadvantages. Ball milling might incorporate some impurities, vapor phase reaction and hydrothermal process require high temperature and pressure, while precipitation is complex and demands long washing and aging times [2].

Chemical synthesis and Sol-gel result the most convenient route to produce ceramic nanoparticles. Sol-Gel method consists in the formation of a sol from alkoxides or organometallic precursors, whose suspended particles polymerize at low temperature. The wet gel generated is then dried and treated thermically [4]. Highly pure particles with large surface area can be obtained by sintering ceramic precursors prepared by Sol-Gel method. Moreover, it is possible to control stoichiometry and morphology, and synthesize materials with required characteristics to suit specific purposes. However, the use of expensive reagents and long gelation times represent important drawbacks for the utilization of this route [3]. Therefore, it is necessary to develop more efficient pathways for obtaining alumina nanopowders by sol-gel method.

Several properties of ceramics are influenced by the stability of precursor colloid solution. The main factors which affect stability are ionic strength, surface charges, pH, temperature and addition of dispersant agents. Particle agglomeration can be prevented through dispersant additives. Organic dispersants improve colloid stability and enhance green densification. Also, temperature required for sintering process decreases. It has been reported that organic compounds rich in carboxyl and hydroxyl groups are the best option for enhancing particle dispersion [5].

Addition of surfactant agents combined with selected stirring times exert a great influence in particle size shape, and agglomeration. Election of a proper dispersant is highly important. For instance, previous reports have informed that better dispersion, smaller particle size and spherical shapes are obtained with SDBS (1/3 benzened disulfonic acid disodium salt) compared to those synthesized using Na(AOT) (Sodium bis-2-ethylhexyl sulfosuccinate). The smallest particles (20-30 nm) were obtained at 48 h of stirring time, using SDBS and thermal treatment of 1200°C [2].

Combustion process is a simple and time saving method for preparing metal oxides, does not require special equipment, uses simple reagents and limits particle agglomeration. Furthermore, this process enhances stabilization of metastable phases and high purity products can be obtained. This synthesis route benefits from redox reactions occurred during combustion (exothermal), so useful materials can be obtained. There are two main processes for nanomaterials synthesis by this technique. The first is Solid State Combustion (SSC) and uses reagents as a compressed pellet. Pellet ignition is achieved using laser, tungsten coil or microwaves. Another route, Solution Combustion (SC), is used for producing different oxide materials. For example, alumina, zirconia and ferrites have been synthesized from precursors solution added with fuel compounds such as urea or glycine [6].

***Corresponding author:** Reyes-López SY, Department of Biological Sciences, Institute of Biomedical Sciences, Autonomous University of Ciudad Juárez, Surrounding Ring of PRONAF and Stockholm s/n, Mexico, Tel: 526566882100; E-mail: simon.reyes@uacj.mx

Received November 09, 2016; **Accepted** November 24, 2016; **Published** December 05, 2016

Citation: Roque-Ruiz JH, Reyes-López SY (2016) Synthesis of α-Al_2O_3 Nanopowders at Low Temperature from Aluminum Formate by Combustion Process. J Material Sci Eng 6: 305. doi: 10.4172/2169-0022.1000305

Combustion occurs in two steps, beginning with formation of ceramic precursor and followed by self-ignition. The latter is achieved through addition of fuel and oxidizing agents. These additives lead an exothermal reaction and form complexes with metal ions, thus hindering particle growth and preventing the particles to agglomerate [7].

Gocmez and Özcan [3] synthesized nanocrystalline α-Al_2O_3 by sol-gel method, using Aluminum nitrate $Al(NO_3)_3$ and carboxylic acids as precursors. First, three different gels were prepared by dissolving aluminum nitrate in tartaric, oxalic and acetic acids, respectively. Next, the samples were dried for 24 h, and heated during 2 h at five different temperatures. According to XRD results, a low intensity γ-Al_2O_3 peak appeared at 800°C. This transitional alumina phase transformed into α-Al_2O_3 at 925°C for the sol-gel obtained using tartaric acid. By contrast, gels synthesized using oxalic and acetic acids showed characteristic diffraction peaks corresponding to α-Al_2O_3 at 950°C. The different temperatures required for producing the highly ordered alumina from amorphous and transitional phases might be caused by the presence of two carboxylic and two hydroxyl groups in tartaric acid chain. These characteristics enhanced the roll of tartaric acid as chelating agent, for it increased its interaction with aluminum ions.

Particle size and morphology of α-Al_2O_3 nanoparticles generated by sol-gel method using aluminum chloride ($AlCl_3$) and aluminum triisopropylate $(C_3H_7O)_3Al$ as inorganic and organic precursors were studied by Rogojan et al., [4]. 0.1 M solution of each precursor was added with NH_3 28% solution, until gel was formed. Then, both gels were aged for 30 and 24 h, respectively, and received thermal treatment. It was reported the presence of gamma and alpha alumina polymorphs at 1000°C in both samples. At higher temperature (1200°C) only alpha alumina was detected. Alumina obtained from the organic compound showed better crystallinity.

A different method that has been used for obtaining alumina nanoparticles is electrode sputtering. An amorphous carbonous matrix with aluminum carbide (Al_4C_3) disperse was synthesized and treated at different temperatures. Matrix decomposition and oxidation of aluminum carbide was achieved by annealing at 950°C [8]. These authors synthesized hollow γ-Al_2O_3 with diameters ranging from 6 to 12 nm, and wall thickness 2 to 3 nm.

Stirring time is an important factor to consider when preparing alumina by sol-gel method. Mirjalili et al., [1] obtained highly dispersed and spherical alumina nanoparticles with mean diameter around 20-30 nm from an aluminum nitrate gel by stirring for 48 h. On the other hand, alumina prepared from gels stirred for 24, 36 and 60 h showed larger particle size and irregular shape. Also, particle agglomeration increased noticeably. The process of particle formation consisted on three stages. In the first step alumina forming reaction occurs, followed by crystallization through a nucleation-growth process during the second step. The last step is particle agglomeration. However, continue stirring kept the solution dispersed and prevented agglomeration. The large particles at 60 h were caused by the increase in concentration due to solvent-loss.

Sharma et al., [7] studied the effect of Urea-Glycine mixtures on the combustion process of nonahydrated aluminum nitrate $Al(NO_3)_3$ $9H_2O$, in order to produce alumina. It was reported that solutions with high urea concentration followed strong exothermic reactions and crystalline phases were obtained. On the other hand, Glycine richer solutions burned at lower temperatures, while an amorphous phase was abundant. The present study was conducted in order to obtain alumina nanopowders using urea and ovalbumin as chelating agents, and compare the effects on particle size and morphology generated by each additive.

Material and Methods

Aluminum formate $Al(O_2CH)_3$ was obtained by chemical synthesis described by Reyes et al., [9] involving a mixture of aluminum with formic acid (HCOOH) using mercuric chloride ($HgCl_2$) as catalyst to obtain the aluminum formate solution which was spray dried to produce fine granulated metal-organic precursor [9,10].

Preparation of Emulsions

Aluminum formate and urea: For the synthesis of alpha alumina nanoparticles, emulsions were prepared from metalorganic precursor aluminum formate and urea aluminum in 3 different weight ratios; 1:1.0, 1:2.0 and 1:3.0 (Table 1), using ethanol as solvent, until obtaining a homogeneous white paste. Heat treatment was done by microwave combustion; each of the emulsions was exposed to microwaves (1000 w) for 5 min to obtain porous agglomerates. The agglomerates were calcined in a muffle furnace at a temperature of 1050°C for one hour in an oxygen rich atmosphere, using a 10°C/min curve. After calcination, the fragile agglomerates were ground in an agate mortar to obtain fine alumina powders (Table 1).

Aluminum formate and ovalbumin: For the synthesis of alpha alumina nanoparticles from aluminum formate and ovalbumin, emulsions were prepared in 3 different weight ratios: 1:1.0, 1:2.0, and 1:3.0, using ethanol as solvent until obtaining a homogeneous white paste (Table 2). Heat treatment was done by microwave combustion. Each of the emulsions was exposed to microwaves (1000 w) for 5 min to obtain porous agglomerates. The agglomerates were calcined in a muffle furnace at a temperature of 1050°C for one hour in an oxygen rich atmosphere, using a ramp of 10°C/min. After calcination, the fragile agglomerates were ground in an agate mortar to obtain fine of alumina powders.

Characterization: Precursor and alumina powders obtained were analyzed using an Attenuated Total Reflection (ATR) technique fitted with a Fourier Transformed (The TENSOR™ 27 series FT-IR spectrometer, ZnSe crystal, Bruker Optics Inc.), while microstructure of calcined powders was studied by SEM (JEOL JSM-6400 SEM, at 15 kV coupled with EDS detector Bruker AXS Inc. XFlash 4010). Crystalline phases were determined by X-ray diffraction (XRD) with a Brucker D8 advance equipment, with Cu Kα radiation (1540 nm), operating at 20 kV with a scan range from 5° to 80° by the powder method.

In order to follow phase transformations of the precursor, 10 mg of sample were run on a thermal analysis instrument (Model Q600 simultaneous differential scanning calorimetry/thermogravimetric

Table 1: Aluminum formate and urea ratios used to obtain alumina.

Sample	$Al(O_2CH)_3$/Urea	$Al(O_2CH)_3$	Urea	Microwave	Temperature
NP-U-1:1	1:1	1 g	1 g	5 min	1050ºC
NP-U-1:2	1:2	5 g	10 g	5 min	1050ºC
NP-U-1:3	1:3	5 g	15 g	5 min	1050ºC

Table 2: Aluminum formate and ovalbumin ratios used to obtain alumina.

Sample	$Al(O_2CH)_3$/ Ovalbumin	$Al(O_2CH)_3$	Ovalbumin	Microwave	Temperature
NP-O-1:1	1:1	1g	1 g	5 min	1050ºC
NP-O-1:2	1:2	2 g	1 g	5 min	1050ºC
NP-O-1:3	1:3	3 g	1 g	5 min	1050ºC

Citation: Roque-Ruiz JH, Reyes-López SY (2016) Synthesis of α-Al_2O_3 Nanopowders at Low Temperature from Aluminum Formate by Combustion Process. J Material Sci Eng 6: 305. doi: 10.4172/2169-0022.1000305

analysis DSC/TGA, TA Instruments). Heating rate was 10 Kmin^{-1} up to 1400°C, with a nitrogen gas flow of 100 cm^3/min.

Results

Aluminum formate: Powders of aluminum formate were characterized by IR-ATR and results are shown in Figure 1 and Table 3, where the characteristic bands of aluminum carboxylate were appreciated. This compound shows vibrations within the range 3300-2500 cm^{-1} due to the structural OH group, and symmetric deformation vibration angle are also observed by the presence of C-H bonds in the molecule, in 2927 and 1094 regions cm^{-1} respectively. Bands also represent asymmetric (COC) links, asymmetric with deformation angle, symmetrical and symmetrical deformation angle in regions 1610, 1416, 1389 and 793 cm^{-1} type vibration respectively, which belong to the orthorhombic coordination. Moreover, there are other three bands corresponding to the carbonyl group in the regions of 772, 656 and 505 cm^{-1} [10,11]. According to DRX results in Figure 2, a high-purity aluminum formate was produced once the solution was spray dried. The crystalline form corresponds to the orthorhombic phase (JCPDS file card no. 38-05839) in agreement with previous works.

Table 3: IR-ATR bands of Aluminum formate obtained by spray drying.

Functional group	Bands (cm^{-1}) According to literature[†]	Bands (cm^{-1}) Experimental
ν (O-H)	3600-2800, 3300-2500	3490, 2356
ν (C-H)	2907, 3100-2800	2927
ν_{as} (O=C-O$^-$)	1620, 1695-1540	1610
ν_{as}, def (O=C-O$^-$)	1400	1416
ν_s (O=C-O$^-$)	1375	1389
ν_{def} (C-H)	1080	1094
$\nu_{s, def}$ (O=C-O$^-$)	800	793
ν (O=C-O$^-$)	775	772
$\nu_{wagging}$ (O=C-O$^-$)	700-450	656, 505

[†][9,11].

Aluminum formate and urea: After obtaining a homogeneous paste of aluminum formate-urea, each sample was exposed to a microwave treatment for 5 min and then analyzed by IR-ATR. As shown in Figure 3, the samples showed a not defined spectrum because of the partial decomposition of formate aluminum and urea, in which ammonia is released as a byproduct (among other gases), showing a decrease in the intensity of the links N-H and a superposition of the bands. However, spectra are dominated by characteristic bands of the carbonyl groups representative of the precursor and the bands corresponding to N-C, C=O and N-H bond of urea, besides of the presence of bands of OH structural groups.

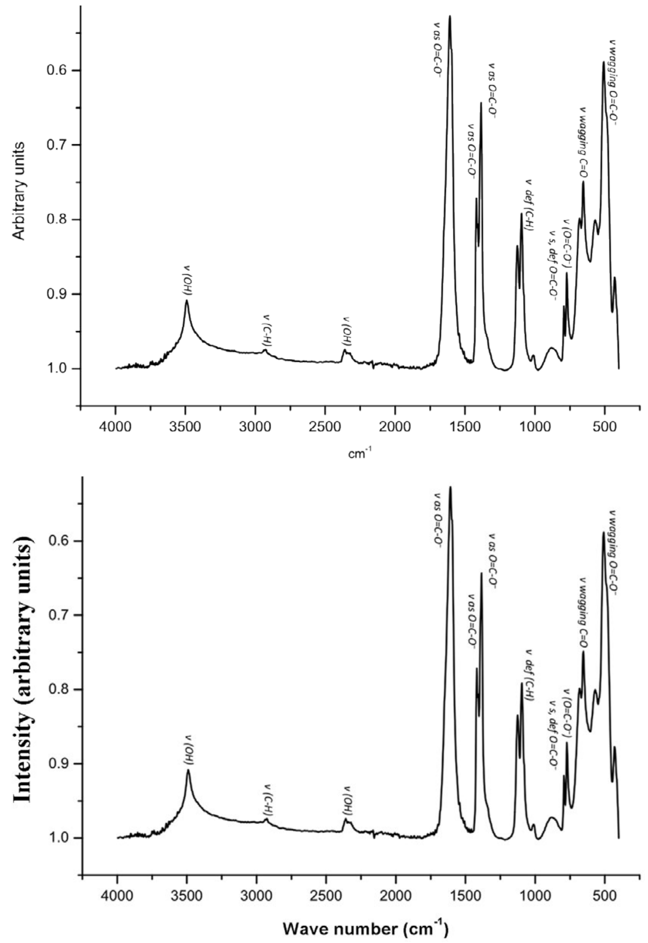

Figure 1: IR-ATR of metalloganic precursor, aluminum formate $Al(CO_2H)_3$.

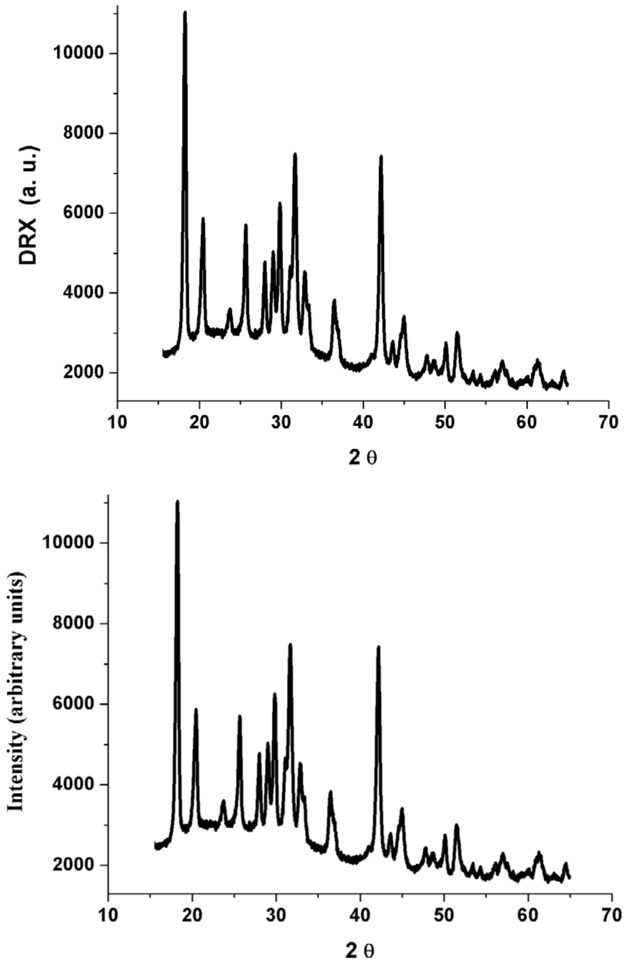

Figure 2: X-Ray diffraction patterns of aluminum formate.

In the ratio 1:1, bands with little intensity of N-H bonds are located in 3433 and 3344 cm^{-1}. The hydroxyl OH group was found to 2259 cm^{-}

^{1}, the bands corresponding to O=C-O bonds were observed in regions 1612, 1353 and 524 cm^{-1}. The C-N bond in 1464 and 1585 cm^{-1}, and C=O group in the region 440-320 cm^{-1} characteristic of urea was also presented. By contrast, in the ratio 1:2 the fainter bands belonging to the N-H group were observed at 3447 and 3342 cm^{-1}, but groups with greater intensity were the O=C-O in the region of 1610, 1353 and 526 cm^{-1}, as well as functional groups C-N in 1581, 1432 and 1585 cm^{-1}, and C=O groups in the region 404-302 cm^{-1}. A band for OH group at 2255 cm^{-1} was also observed. For the ratio 1:3, N-H bonds at 3435 and 3342 cm^{-1} appeared, the predominant bands were recorded in 1638, 1343 and 526 cm^{-1} for the O=CO- group, also the C-N functional groups is observed at 1581 and 1343 cm^{-1} and the C=O bands is recorded at 763 and 404-306 cm^{-1}. The band of OH group was identified at position 2262 cm^{-1}. IR vibration bands identified in this study are shown in Table 2.

Results showed a tendency, in which bigger amounts of urea remained in samples obtained from emulsions with higher aluminum formate/fuel ratio. Probably, the heat generated during microwave-aided combustion was not enough to decompose this reagent into ammonia and carbon dioxide. Porous and fragile aggregates obtained from emulsions allow the generation of fine powders after calcining and milling processes.

Figure 4 shows IR spectra of samples at different weight ratio after calcining treatment at 1050°C for 1 h. Bands corresponding to O-Al-O bonds characteristic of alpha alumina polymorph (octahedral structure AlO_6) are present in all samples. Vibration bands of sample from ratio 1:1.0 are present at 379, 491, 565 and 633 cm^{-1}. Ratio 1:2.0 showed wider and less defined bands, yet they were located alike to the previous sample (381, 487, 567 and 634 cm^{-1}). Similarly, bands at 381, 488, 566 and 634 cm^{-1} are present in sample with 1:3.0 weight ratio. However, gamma (tetrahedral AlO_4) and theta (octahedral AlO_6) transition phases are also present in the last two samples (bands between 400 and 800 cm^{-1}) and cannot be differentiated by IR technique [9,11-14]. In addition, differences in band intensities between the three samples obtained from their respective precursor/fuel ratios are influenced by the crystalline structure. The higher intensity in the first sample (1:1 ratio) is due to the abundance of α-Al_2O_3 phase, while lesser bands (1:2 and 1:3 ratios) were generated by the competence of alpha and gamma phases for nucleation sites (according to XRD results in Figure 5). This effect was more remarkable in sample at 1:2 ratio, while samples with higher urea content (1:3 ratio) showed sharper bands due to phase stabilization and increased proportion of α-Al_2O_3. Also, theta polymorph is unstable and reactive, so it transforms directly into alpha alumina at 1000°C [10]. All vibration bands discussed are shown in Tables 4 and 5.

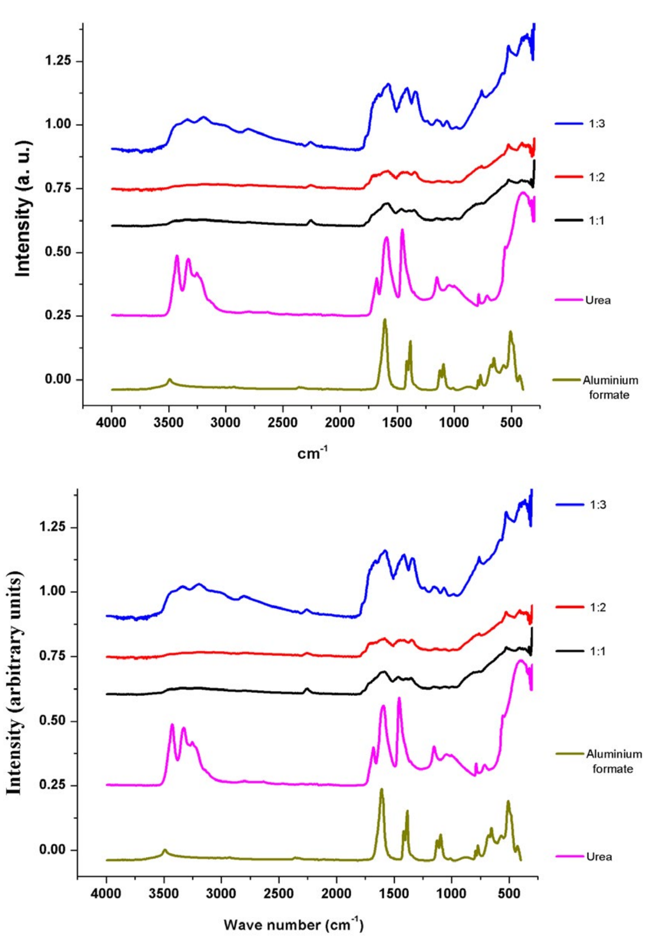

Figure 3: IR-ATR spectra of precursor/urea samples after microwave treatment in 1:1.0, 1:2.0 and 1:3.0 ratios.

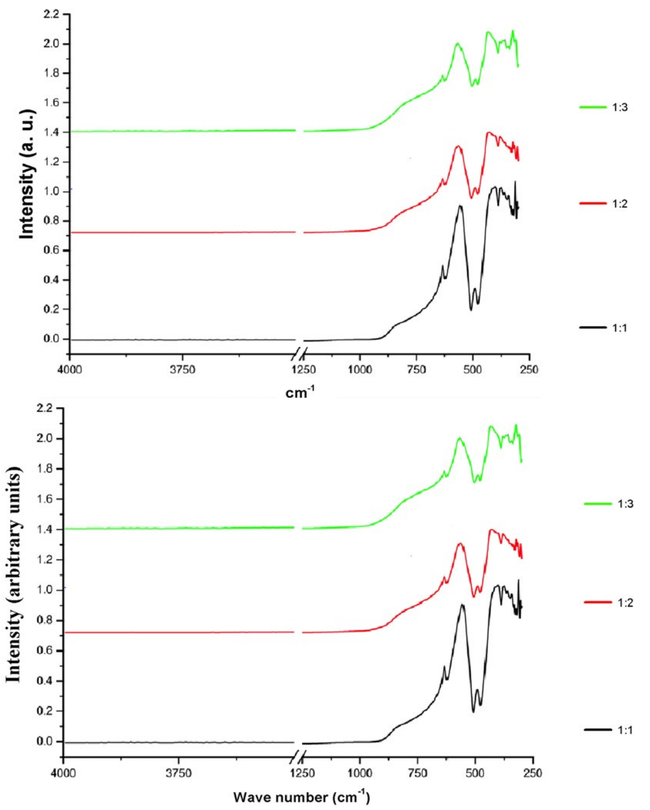

Figure 4: IR-ATR alumina spectra of samples in 1:1.0, 1:2.0 and 1:3.0 ratios.

Each ratio was characterized by XRD (Figure 5) in order to determine the effects of urea content on phase transformation. Defined diffraction peaks representing alpha alumina are present in sample with 1:3 ratio, along with fewer peaks generated by theta and gamma phases. By contrast, sample with 1:2 y 1:1 ratios showed higher crystallinity as a result of competence for nucleation sites between alpha and gamma alumina phases. In sample with 1:1 ratio, only well-defined alpha alumina peaks were identified, according to γ [96-101-

Table 4: IR bands of emulsions after receiving microwave thermal treatment.

Functional group	Wavenumber (cm^{-1})	1:1.0 ratio	1:2.0 ratio	1:3,0 ratio
v (O-H)	Literature [†]	3300-2500	3300-2500	3300-2500
	Experimental	3259	3262	3259
v (N-H)	Literature [†]	3437, 3350, 3325, 3200	3437, 3350, 3325, 3200	3437, 3350, 3325, 3200
	Experimental	3433, 3427, 3344, 3325	3435, 3427, 3342, 3325	3457, 3427, 3434,3325
v as (O=C-O^-)	Literature [†]	1620, 1695-1540	1620, 1695-1540	1620, 1695-1540
	Experimental	1612	1638	1638
v (C-N)	Literature [†]	1420-1400	1420-1400	1420-1400
	Experimental	1454, 1464	1454, 1413	1454, 1412
v (O=C-O^-)	Literature [†]	1360	1360	1360
	Experimental	1353	1343	1346
v (C-N)	Literature [†]	1660-1620	1660-1620	1660-1620
	Experimental	1590, 1585	1590, 1581	1590, 1583
v (O=C-O^-)	Literature [†]	700-450	700-450	700-450
	Experimental	524	526	528
v (C=O)	Literature [†]	1670-1650, 700-500 390-305	1670-1650, 700-500 390-305	1670-1650, 700-500 390-305
	Experimental	1679, 711 440-320	1670, 711 404-306	1679, 711 404-318
v (C-N)	Literature [†]		700-500	700-500
	Experimental		763	759
v_{as} (N-C-N)	Literature [†]	1360-1300	1360-1300	1360-1300
	Experimental	1335	1335	1335
v_{as} (N-C-N)	Literature [†]	1190-1140	1190-1140	1190-1140
	Experimental	1154	1154	1154
v (O=C-N)	Literature [†]	695-550	695-550	695-550
	Experimental	554	554	554

[†][9,11].

Table 5: IR bands present in alumina samples obtained by calcinations at 1050°C/1 h.

Key/code	Bands (cm^{-1})reported in literature [†]:	Experimental Bands (cm^{-1}):	Bond type
NP-U-1:1 (1:1.0 ratio)	385	379	AlO_6 bending
	484, 495	491	AlO_6
	567, 569	565	AlO_6
	634, 635	633	AlO_6
	400-800	400-800	AlO_4, AlO_6
NP-U-1:2 (1:2 ratio)	385	381	AlO_6 bending
	484, 495	487	AlO_6
	567, 569	567	AlO_6
	634, 635	634	AlO_6
	400-800	400-800	AlO_4, AlO_6
NP-U-3.0 (1:3 ratio)	385	381	AlO_6 bending
	484, 495	488	AlO_6
	567, 569	566	AlO_6
	634, 635	634	AlO_6
	400-800	400-800	AlO_4, AlO_6

[†] [9,11-14].

0462]; η [96-120-0016]; α [96-100-0018]; θ [96-120-0006] diffraction cards. In samples obtained from 1:1.0 and 1:2.0 precursor/urea ratios, fuel promoted aluminum formate decomposition and complete transition into α-alumina phase. On the other hand, increasing fuel rate to 1:3.0 promoted the transition into γ and θ-alumina polymorphs. Probably, the excess of urea protected Al^{+3} ions from complete oxidation, thus obtaining transitional alumina phases with FCC structure instead of HCP.

Particle size distribution by DLS

As shown in Figure 6 and Table 6, nanometric particles were synthesized from the three precursor/fuel ratios employed. The lowest diameters (71.43 nm ± 33.25) belonged to particles obtained by calcining samples with 1:3 ratios, resulting in α-alumina nanopowders. Micrometric particles were present as a result of interactions between Al^{+3} ions, for there was not enough urea in samples in order to inhibit grain nucleation [15,16]. Also, diameter increased because different phases competed for nucleation centers, promoting an uncontrolled formation of O-Al-O bonds. Particle was strongly influenced by precursor/urea ratio and by microwave thermal treatment as well. The higher urea concentration protected aluminum cations from crystal growth, resulting in shorter diameters [15,16]. Microwave treatment originated sample dehydration and generation of a fragile porous carbonous material, which was ground in fine denser powders after calcination [17,18].

Scanning electron microscopy

The micrograph of sample obtained from 1:1.0 ratios in Figures 7a-c shows circular alumina particles with nanometric size (Figure 7). During decomposition, aluminum formate tends to transform into micrometric acicular α-alumina structures approximately 200 nm, as reported in 2013[10]. This shape differs from the acicular morphology reported previously in 2013 [10]. This difference was due to the addition of urea, which worked as a protector material, preventing particle growth in C axis. Only nanometric alumina particles with regular round morphology were observed, which is also confirmed by DLS results. Micro-elemental analysis carried out by EDX demonstrated that 61.64 wt% and 38.35 wt% of sample consists in oxygen and aluminum. Therefore, there were not impurities detected in alpha

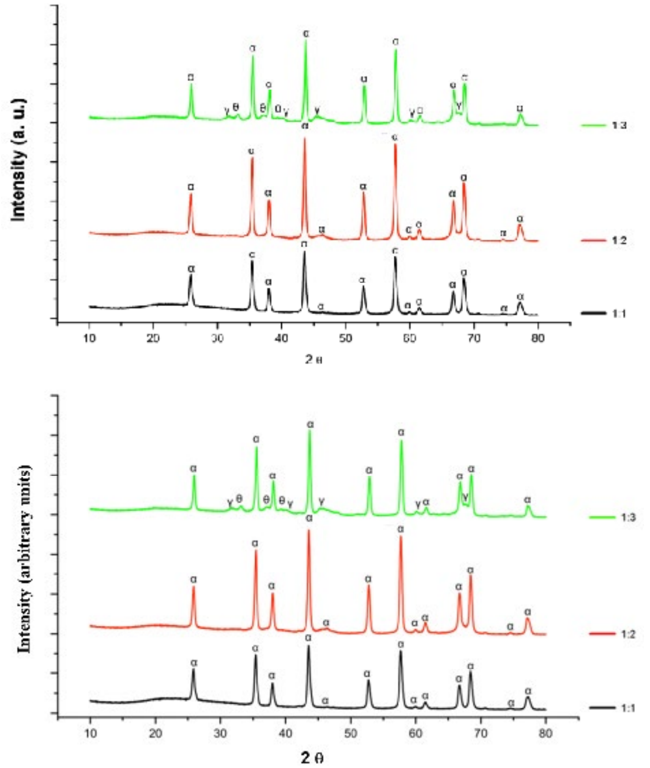

Figure 5: Diffractograms of alumina samples in 1:1.0, 1:2.0 and 1:3.0 ratios, calcined at 1050°C for 1 h.

Citation: Roque-Ruiz JH, Reyes-López SY (2016) Synthesis of α-Al_2O_3 Nanopowders at Low Temperature from Aluminum Formate by Combustion Process. J Material Sci Eng 6: 305. doi: 10.4172/2169-0022.1000305

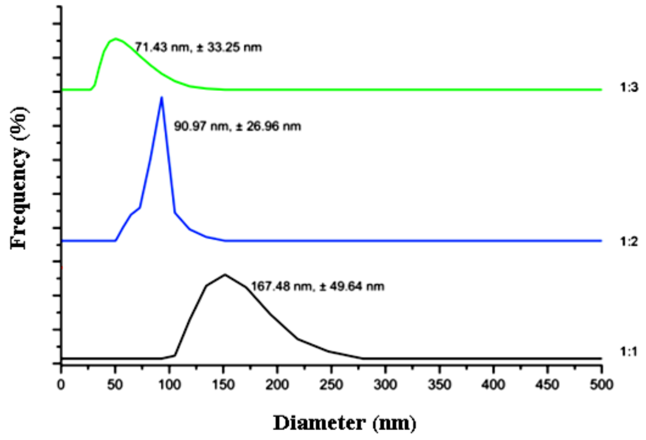

Figure 6: Particle size distribution of alumina samples calcined at 1050°C for 1 h.

Table 6: Statistical data for diameters of alumina particles obtained from alumina samples prepared from different precursor/urea ratios.

Key/Code	Mean (nm)	Standard deviation (nm)	Mode (nm)
NP-U-1:1	167.48	49.69	171.25
NP-C-1:2	90.97	26.96	82.33
NP-C-1:3	71.43	33.25	50.53

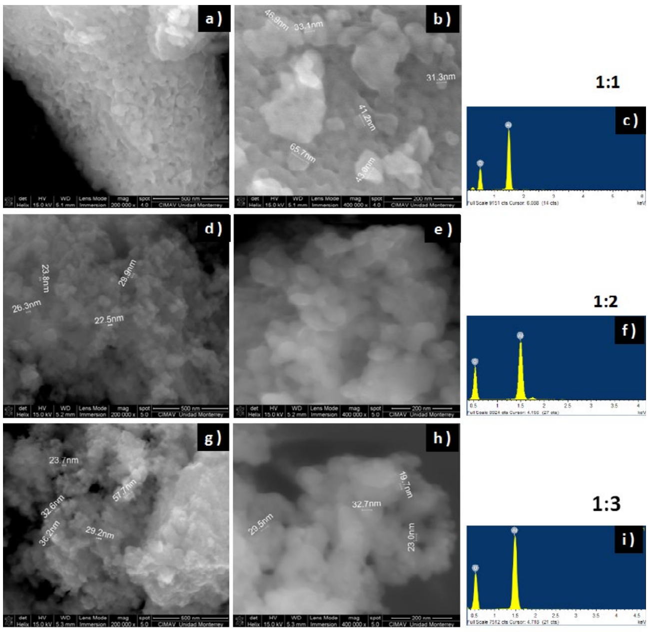

Figure 7: Micrographs of alumina samples obtained from precursor/urea ratios at 1050°C for 1h: a) 200,000x, b) 400,000x and c) EDX analysis for 1:1 ratio; d) 200,000x, e) 400,000x and f) EDX analysis for 1:2 ratio and g) 200,000x, h) 400,000x and i) EDX analysis for 1:3 ratio.

alumina synthesized at these conditions. Agglomerations of α-alumina particles prepared by calcinations of samples with 1:2 precursor/urea ratios were observed in Figures 7d and e. Similarly to previous example, particle agglomeration and growth in C axis was prevented by the urea amount added to ceramic precursor. Impurities were not detected, according to EDX results. Only regular nanometric particles were observed in alumina sample from 1:3.0 ratios in Figures 7f and g. EDX analysis demonstrated the high purity of synthesized alumina, which was composed by 66.53% Oxygen and 33.47% Aluminum.

Other authors [16] obtained 50-100 nm particle aggregates with a narrow unimodal distribution (50.7 nm ± 17.55). Urea was chosen as fuel because it allows the generation of dense powders free of carbon residues and other impurities when compared to other reagents, such as glycine [19].

Aluminum formate and ovalbumin: The particles obtained from aluminum formate-ovalbumin using ethanol as solvent presented fragile consistency with fine particles. Emulsions exposed to microwave treatment during 5 min increased hardness and presented a more solid appearance. Microwave treatment aided solvent evaporation, since during this stem temperature increased until 200°C/min. After thermal treatment during 1 h, porous and fragile aggregates obtained from emulsions allow the generation of fine powders after calcining and milling processes. During heating process a characteristic sulfur odour was perceived, which was produced by the decomposition of sulfhydryl groups in ovalbumina.

The alumina powders from aluminum formate-ovalbumin analyzed by IR-ATR are shown in Figure 8, the samples showed a not defined spectrum, for the partial decomposition of formate aluminum and ovalbumin. Vibration bands corresponding to precursor/ovalbumin emulsions, and representing transition into alumina are shown in Figure 8. Carboxyl representative bands diminished during

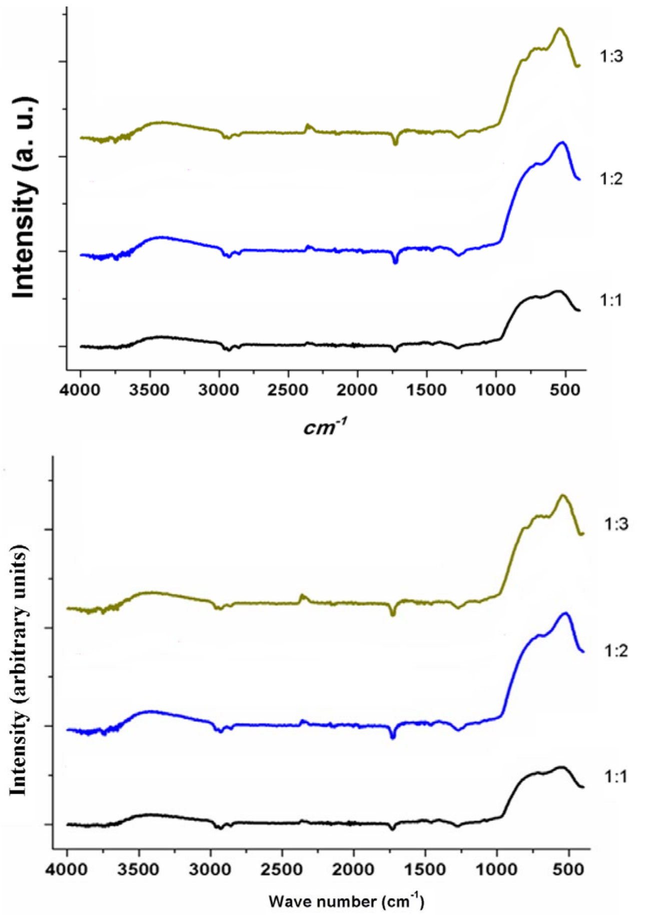

Figure 8: IR spectra of $Al(COOH)_3$/Ovalbumin emulsions calcined at 1050°C.

this transition as a result of precursor/ovalbumin transformation in different alumina polymorphs. Bands representing amorphous alumina phase are located at 710 and 548 cm^{-1}, as shown in Figure 8, while η-alumina (JCPS File Card No. 4-185) phase vibration bands were observed at 518 and 510 cm^{-1}. Characteristic α-alumina (JCPS File Card No. 10-0173) vibration bands are located at 650 and 495 cm^{-1}. Figure 9 shows X-ray diffraction patterns of alumina powders obtained by calcinning (1050°C) samples from an emulsion of Aluminum formate/Ovalbumin in Ethanol. Transitions from ceramic precursor to η and α-alumina polymorphs were detected.

Each ratio was characterized by XRD in Figure 9 in order to determine the effects of ovalbumin content on phase transformation. Defined diffraction peaks representing alpha alumina are present in sample with 1:1 ratio, along with fewer peaks generated by theta and gamma phases. By contrast, sample with 1:2 y 1:3 ratios showed lower crystallinity as a result of competence for nucleation sites between alpha, tetha and gamma alumina phases. In sample with 1:1 ratio, only well-defined alpha alumina peaks were identified, according to γ [96-101-0462]; η [96-120-0016]; α [96-100-0018]; θ [96-120-0006] diffraction cards. In samples obtained from 1:2 and 1:2 precursor/ovalbumin ratios, fuel promoted aluminum formate decomposition and complete transition into α-alumina phase. On the other hand, increasing fuel rate to 1:3.0 promoted the transition into γ and θ-alumina polymorphs. Probably, the excess of ovalbumin protected Al^{+3} ions from complete oxidation, thus obtaining transitional alumina phases with FCC structure instead of HCP in the same route, as in urea.

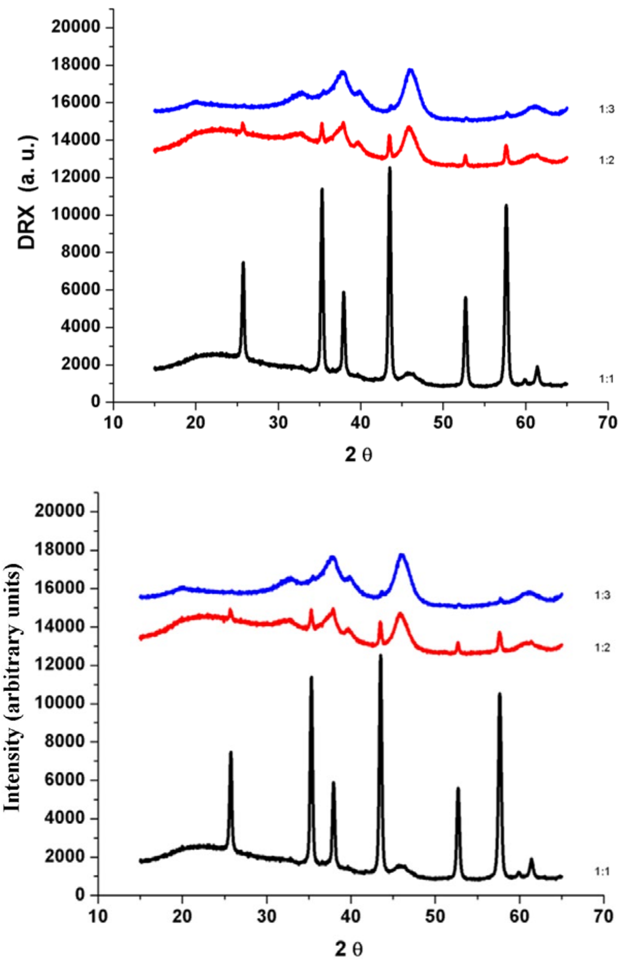

Figure 9: Diffractogram of alumina powders obtained by calcination (1050°C) of three Aluminum formate/Ovalbumin emulsions.

Table 7 shows data concerning to mean diameter for alumina particles obtained from samples with different Aluminum formate/Ovalbumin ratios and repetitions. Least diameter (62.76 nm) corresponded to sample with 1:3.0 ratio, while longest diameter was obtained from sample with 1:1 ratio (91.78 nm).

Median diameter value obtained by DLS was 95.9 nm for alumina powders obtained from samples in 1:1 precursor/ovalbumin ratio (NP-O-1:1), as shown in Figure 10. Mean particle diameter was 91.78 ± 21.72 nm, while mode was 88.5 nm. Particle size statistical data for sample NP-O-1:2, mean alumina particle size was approximately 84.51 ± 24.82 nm, while median and mode were 84.59, according to DLS data.

Scanning Electron Microscopy

The micrograph of sample obtained from 1:1.0 ratio in Figures 11a and 11b shows circular alumina particles with nanometric size. During decomposition, aluminum formate tends to transform into micrometric acicular α-alumina structures approximately 200 nm, as reported in 2013 [10]. Nanometric alumina particles with regular round morphology were observed with the increment of ovalbumin, which is also confirmed by DLS results. Micro-elemental analysis carried out by EDX demonstrated that the all sample consists in oxygen and aluminum. Therefore, there were not impurities present in alpha alumina synthesized at these conditions. Similarly to previous urea example, particle agglomeration and growth in C axis was prevented by the ovalbumin amount added to ceramic precursor.

Conclusions

IR and XRD spectra demonstrate that gamma, eta and alpha alumina phases are present in samples after calcining for 1 h at 1050°C and these results suggest that these carboxylates are useful precursors

Table 7: Particle size statistical data, mean diameter, and standard deviation for alumina obtained from samples at different Aluminum formate/Ovalbumin ratio.

Key/Code	Mean (nm)	Standard deviation (nm)
NP-O-1:1	91.78	21.72
NP-O-1:2	84.51	24.82
NP-O-1:3	62.76	25.9

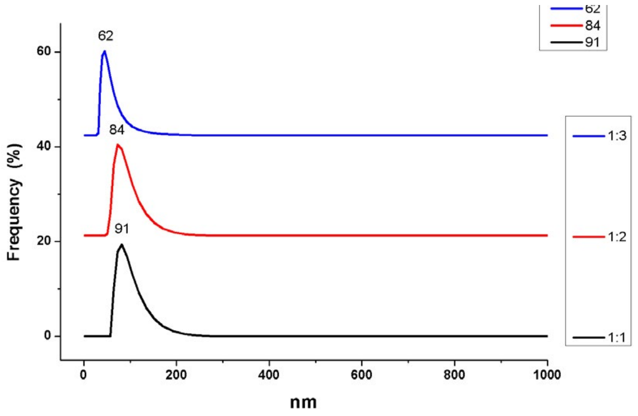

Figure 10: Particle size distribution of alumina samples calcined at 1050°C for 1 h, for Aluminum formate/Ovalbumin emulsions.

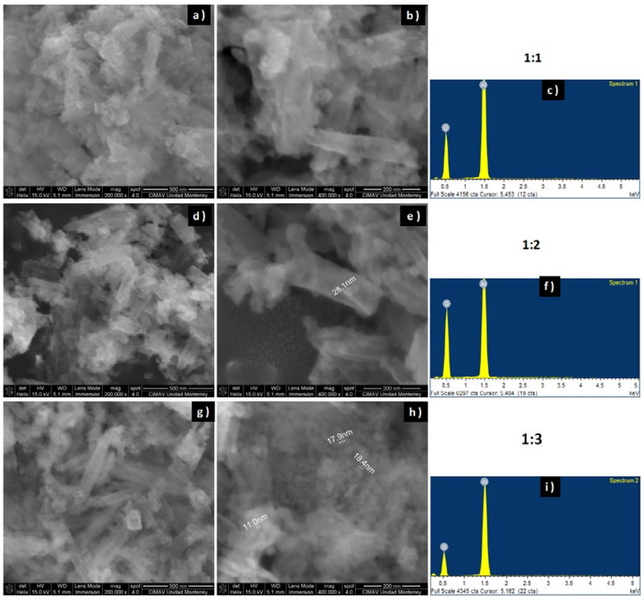

Figure 11: Micrographs of alumina samples obtained from precursor/Ovalbumin ratios at 1050°C for 1h: a) 200,000x, b) 400,000x and c) EDX analysis for 1:1 ratio; d) 200,000x, e) 400,000x and f) EDX analysis for 1:2 ratio and g) 200,000x, h) 400,000x and i) EDX analysis for 1:3 ratio.

to produce α-alumina powders at relatively low temperature. Using different emulsion ratios (formate/urea and formate/ovalbumin), it was concluded that the best emulsion ratio was 1:3 due the obtaining of pure nano alpha alumina with a mean size 30-90 nm with spherical morphology.

Nano spherical α-Al_2O_3 particles were produced using a metalorganic route with a calcination temperature of 1050ºC for 1 h, which makes it a highly competitive option when compared to others methods employed to obtain this material, reducing complexity and processing time.

Acknowledgements

Bachelor students Fabiola Alejandra Mejía-Reyes and Alexis Guillermo Mijares-Alvarado (UACJ). Dr. Eduardo Martínez-Guerra (CIMAV). PROMEP, CONACyT and Universidad Autónoma de Ciudad Juárez for funding this project.

References

1. Mirjalili F, Abdullah LC, Mohamad H, Fakhru'l-Razi A, Dayang Radiah AB, et al. (2011) Process for producing nano-alpha-alumina powder. ISRN Nanotechnology 2011: 1-5.
2. Mirjalili F, Hasmaliza M, Abdullah LC (2010) Size-controlled synthesis of nano α-alumina particles through the sol-gel method. Ceram Int 36: 1253-1257.
3. Gocmez H, Özcan O (2008) Low temperature synthesis of nanocrystalline α-Al_2O_3 by a tartaric acid gel method. Mater Sci Eng A 475: 20-22.
4. Rogojan R, Andronescu E, Ghitulica C, Vasile BS (2011) Synthesis and characterization of alumina nano-powder obtained by sol-gel method. UPB Sci Bull Series B 73: 67-76.
5. 5 Gocmez H (2006) The interaction of organic dispersant with alumina: A molecular modelling approach. Ceram int 32: 521-525.
6. Patil KC, Aruna ST, Mimani T (2002) Combustion synthesis: an update. Curr Opin Solid State Mater Sci 6: 507-512.
7. Sharma A, Rani A, Singh A, Modi OP, Gupta GK (2014) Synthesis of alumina powder by the urea–glycine–nitrate combustion process: a mixed fuel approach to nanoscale metal oxides. Applied Nanoscience 4: 315-323.
8. Smovzh DV, Kalyuzhnyi NA, Zaikovsky AV, Novopashin SA (2013) Synthesis of hollow nanoparticles γ-Al_2O_3. Adv Nanoparticles 2: 120-124.
9. López SR, Rodrıguez JS, Sueyoshi SS (2006) Low-temperature formation of alpha alumina powders via metal organic synthesis. Azo J of Materials Online 2.
10. Reyes-López SY, Acuñaa RS, López-Juárez R, Rodríguez JS (2013) Analysis of the phase transformation of aluminum formate Al (O2CH) 3 to α-alumina by Raman and infrared spectroscopy. J Ceram Process Res 14: 627-631.
11. Socrates G (1994) Infrared and Raman characteristic group frecuencies: tables and charts.(3rd Ed) John Wiley & Sons Ltd, USA.
12. Kim JH, Yoo SJ, Kwak DH, Jung HJ, Kim TY, et al. (2014) Characterization and application of electrospun alumina nanofibers. Nanoscale Res Lett 9: 1-6.
13. Boumaza A, Favaro L, Lédion J, Sattonnay G, Brubach JB, et al.(2009)Transition alumina phases induced by heat treatment of boehmite: An X-ray diffraction and infrared spectroscopy study. J Solid State Chem 182: 1171-1176.
14. Barker AS (1963) Infrared lattice vibrations and dielectic dispersion in corundum. Phys Rev 132: 1475-1481.
15. Septawendar R, Suhanda Edwin F (2011) Nanocrystalline α-Al_2O_3 powder preparation with sucrose as a template through a chemical route. J Ceram Process Res 12: 365-370.
16. Lee YC, Wen SB, Wenglin L, Lin CP (2007) Nano α-Al_2O_3 Powder Preparation by Calcining an Emulsion Precursor. J Am Ceram Soc 90: 1723-1727.
17. Prado-Gonjal J, Morán E (2011) Síntesis asistida por microondas de sólidos inorgánicos. An Quím 107: 129-136.
18. Mangalaraja RV, Mouzon J, Hedström P, Camurri CP, Ananthakumar S, et al. (2009) Microwave assisted combustion synthesis of nanocrystalline yttria and its powder characteristics. Powder Technol 191: 309-314.
19. Zhuravlev VD, Bamburov VG, Beketov AR, Perelyaeva LA, Baklanova IV, et al. (2013)Solution combustion synthesis of α-Al_2O_3 using urea. Ceram Int 39: 1379-1384.